1-1-2016

A Strategy for configuration of an integrated flexible sulfur cathode for high-performance lithium-sulfur batteries

Hongqiang Wang
University of Wollongong, hw571@uowmail.edu.au

Wenchao Zhang
University of Wollongong, wz990@uowmail.edu.au

Hua-Kun Liu
University of Wollongong, hua@uow.edu.au

Zaiping Guo
University of Wollongong, zguo@uow.edu.au

A Strategy for configuration of an integrated flexible sulfur cathode for high-performance lithium-sulfur batteries

Abstract

Lithium-sulfur batteries are regarded as promising candidates for energy storage devices owing to their high theoretical energy density. The practical application is hindered, however, by low sulfur utilization and unsatisfactory capacity retention. Herein, we present a strategy for configuration of the sulfur cathode, which is composed of an integrated carbon/sulfur/carbon sandwich structure on polypropylene separator that is produced using the simple doctor-blade technique. The integrated electrode exhibits excellent flexibility and high mechanical strength. The upper and bottom carbon layers of the sandwich-structured electrode not only work as double current collectors, which effectively improve the conductivity of the electrode, but also serve as good barriers to suppress the diffusion of the polysulfide and buffer the volume expansion of the active materials, leading to suppression of the shuttle effect and low self-discharge behavior. An integrated flexible sulfur cathode consisting of a carbon/sulfur/carbon sandwich structure coated on a polypropylene separator was prepared by the doctor-blade method. This sulfur cathode could enhance the electronic conductivity, toleration of volume expansion, and control of the polysulfide diffusion, thereby improving the electrochemical performance of lithium-sulfur batteries.

Keywords

configuration, strategy, performance, high, batteries, cathode, integrated, sulfur, lithium, flexible

Disciplines

Engineering | Science and Technology Studies

Publication Details

Wang, H., Zhang, W., Liu, H. & Guo, Z. (2016). A Strategy for configuration of an integrated flexible sulfur cathode for high-performance lithium-sulfur batteries. Angewandte Chemie International Edition, 55 (12), 3992-3996.

A Strategy for Configuration of an Integrated Flexible Sulfur Cathode for High-Performance Lithium-Sulfur Batteries

Hongqiang Wang, Wenchao Zhang, Huakun Liu, and Zaiping Guo*

Abstract: Lithium-sulfur batteries are regarded as promising candidates for energy storage devices due to their high theoretical energy density. The practical application is hindered, however, by low sulfur utilization and unsatisfactory capacity retention. Herein, we present a novel strategy for configuration of the sulfur cathode, which is composed of an integrated carbon/sulfur/carbon sandwich structure on polypropylene separator that is produced via the simple doctor blade technique. The integrated electrode exhibits excellent flexibility and high mechanical strength. The upper and bottom carbon layers of the sandwich-structured electrode not only work as double current collectors which effectively improve the conductivity of the electrode, but also serve as good barriers to suppress the diffusion of the polysulfide and buffer the volume expansion of the active materials, leading to suppression of the shuttle effect and low self-discharge behavior.

Lithium-sulfur (Li-S) batteries show great potential for the next generation of lithium-ion batteries, as sulfur features high theoretical capacity (1675 mAh g^{-1}), high specific energy density (2600 Wh kg^{-1}), cost effectiveness, and nontoxicity.[1-3] Nevertheless, the broad application of Li-S batteries is limited by several persistent problems, including the low electronic conductivity of sulfur and its discharge product, the high solubility and diffusivity of polysulfide intermediates, and the related side reaction “shuttle effect”, as well as volume expansion caused by the intercalation of Li into the sulfur.[4-7] Therefore, the key points for the development of Li-S batteries are to improve the conductivity of the sulfur cathode, enhance the tolerance for volume expansion, maintain the soluble polysulfides within the cathode region. In the past few years, much effort has been devoted to addressing these issues by constructing nanostructured sulfur cathodes, confining the sulfur within a conductive framework, such as nanoporous carbon,[8-12] graphene,[13,14] conductive polymer,[15-17] and metal oxides.[5,18-21] Although employing a matrix to constrain the sulfur could significantly improve the conductivity and alleviate the dissolution of polysulfides, there is still a significant amount of polysulfides dissolved into the electrolyte, especially under long cycling and high sulfur loading. Recently, novel configurations of Li-S cell have been considered as an alternative approach to address the shuttle effect.[22-27] Many advanced interlayers fabricated from microporous carbon,[23] carbon nanotubes,[24] carbon nanofibers,[25] and graphene oxide [26] have been inserted between the cathode and separator in the cell configuration, which could greatly decrease the charge transfer resistance and trap the soluble polysulfides, resulting in improved utilization efficiency of the active materials and enhanced cyclability of batteries. On the other hand, functionalizing the separator in Li-S batteries is also an effective route to preventing the diffusion of polysulfides across the separator. This can be achieved by introducing a coating layer on the cathode side of separator, such as with Nafion-coated, carbon-coated and graphene-oxide-coated separators.[28-30] A complicated synthesis process and additional cost would be introduced in applying these strategies, however, so a much simpler and more cost effective construction would be more desirable for the large-scale fabrication and real application.

Inspired by this need, herein, we have designed for the first time an integrated flexible cathode architecture consisting of carbon/sulfur/carbon sandwich structure spread directly on a polypropylene (PP) separator (CSC@separator) via the simple doctor blading technique, in which commercial sulfur and Super P carbon (surface area of 64.56 m^2 g^{-1}, Figure S1) are used as the raw materials to be directly coated on the PP separator as the sulfur layer and carbon layer, respectively.

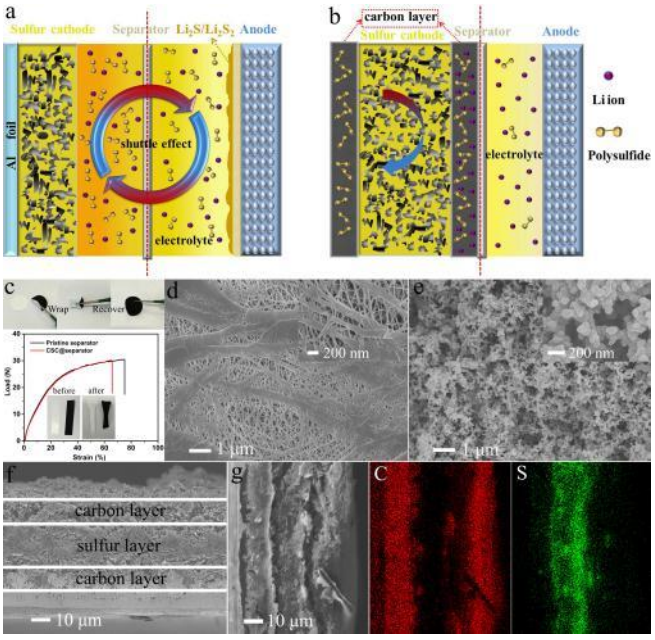

Figure 1. Schematic illustration of Li-S cells configuration employing a) conventional electrode and b) integrated sandwich structured electrode. c) Digital photographs and load-strain curves of pristine separator and CSC@separator electrode, demonstrating excellent flexibility and high mechanical strength. SEM images of the surface of d) the pristine separator and e) the CSC@separator electrode. f) Cross-section of CSC@separator electrode and g) corresponding elemental mapping.

A schematic illustration of the cell configuration using a conventional electrode and the CSC@separator electrode is

[*] H.Q. Wang, Prof. Z.P. Guo
Hubei Collaborative Innovation Centre for Advanced Organic Chemical Materials, Ministry of Education Key Laboratory for the Synthesis and Application of Organic Functional Molecules & College of Chemistry and Chemical Engineering
Hubei University, Wuhan 430062, PR China
E-mail: zguo@uow.edu.au
H.Q. Wang, W.C. Zhang, Prof. H.K. Liu, Prof. Z.P. Guo
Institute for Superconducting & Electronic Materials
University of Wollongong
NSW 2500, Australia

Supporting information for this article is given via a link at the end of the document ((Please delete this text if not appropriate))

shown in Figure 1a, b. Compared to the conventional electrode configuration, the CSC@separator electrode, where the CSC sandwich layers are directly coated on separator without usage of aluminium (Al) foil as substrate, greatly reduces the weight of the electrode (the weight of the substrate is reduced by 78%, 1.13 mg cm^{-2} for the separator and 5.30 mg cm^{-2} for Al foil) and exhibits excellent flexibility. The two carbon layers next to the sulfur layer could not only act as double current collectors from top to bottom to accelerate electron transport into the active material, but also serve as physical barriers to buffer the volume changes during cycling, preventing active material exfoliation and maintaining the integrity of the whole electrode. In addition, the double carbon coating layers work as effective reservoir to trap the dissolved polysulfides within the cathode region, without affecting the lithium ion diffusion (Figure S2), resulting in suppression of the shuttle effect and improved long-lasting cycling stability. Lastly, the utilization of commercial sulfur powders and Super P carbon as raw materials and the mature doctor blade process make it an easy, low-cost, and scalable approach.

The as-prepared integrated CSC@separator electrode shows excellent flexibility, strong adhesion, and high mechanical strength (Figure 1c). The bare separator displays a highly nanoporous structure with pore size around several hundred nanometers (Figure 1d). In contrast, the CSC@separator electrode shows nanoparticle clusters on one side (Figure 1e), while the other side of the electrode still keeps its nanoporous structure (Figure S3). The loose structure of the carbon coating layer ensures that the liquid electrolyte penetrates easily into the whole sandwich structure and so that the electrochemical reactions proceed. The sandwich structure of the electrode can be further examined in the cross-sectional scanning electron microscope (SEM) image (Figure 1f). The sandwich structure strongly adheres to the separator as an integrated electrode. The thicknesses of the carbon coating layers and the sulfur layer are about 10 µm and 20 µm, respectively. The elemental mapping results (Figure 1g) clearly confirm the layered carbon/sulfur/carbon sandwich structure. The weight of two carbon layers is around 0.38-0.52 mg cm^{-2}, much lighter than the weight of the sulfur layer at 1.0-1.4 mg cm^{-2}. Even including the weight of the carbon coating layers, the content of sulfur in the whole electrode is still around 50%.

To demonstrate the effectiveness of integrated CSC@separator electrode, a series of electrodes were prepared for comparison, including a sulfur layer, a dual sulfur/carbon layer, and a dual carbon/sulfur layer coated on the separator (S@separator, SC@separator, CS@separator, respectively), and the same sulfur content mixed with Super P and binder coated on Al foil (S@Al foil). The area of integrated electrode is the same as that of S@Al foil electrode. As shown in Figure 2a, surprisingly, all integrated separator electrodes show enhanced utilization efficiency of sulfur and cycling stability at 0.2 C (1 C = 1000 mA g^{-1}), compared to the S@Al foil electrode. The CSC@separator electrode shows the highest reversible capacity and the best cycling stability, which is attributed to the integrated structure of the electrode and decreased charge transfer resistance (Figure 2b). Furthermore, the CSC@separator electrode shows overlapping voltage plateaus and lower polarization compared to the S@Al foil electrode (Figure 2c, d). The charge-discharge potential difference (ΔE) of the cells with CSC@separator electrode remains almost constant with cycle number, while the ΔE increases with cycling for the cell with S@Al foil electrode (Figure S4). A similar tendency for ΔE can be observed when the cells are tested at different current densities (Figure S5), indicating improved redox reaction kinetics and reversibility of the system. It was reported that the upper discharge plateau at 2.3 V represents the reduction reaction from sulfur to high-order soluble polysulfides.[29] Therefore, the high retention rate of discharge capacity (Q_H) (Figure S6), corresponding to the upper plateau for the CSC@separator electrode, indicates that the carbon coating layers have strong polysulfide-trapping capability.

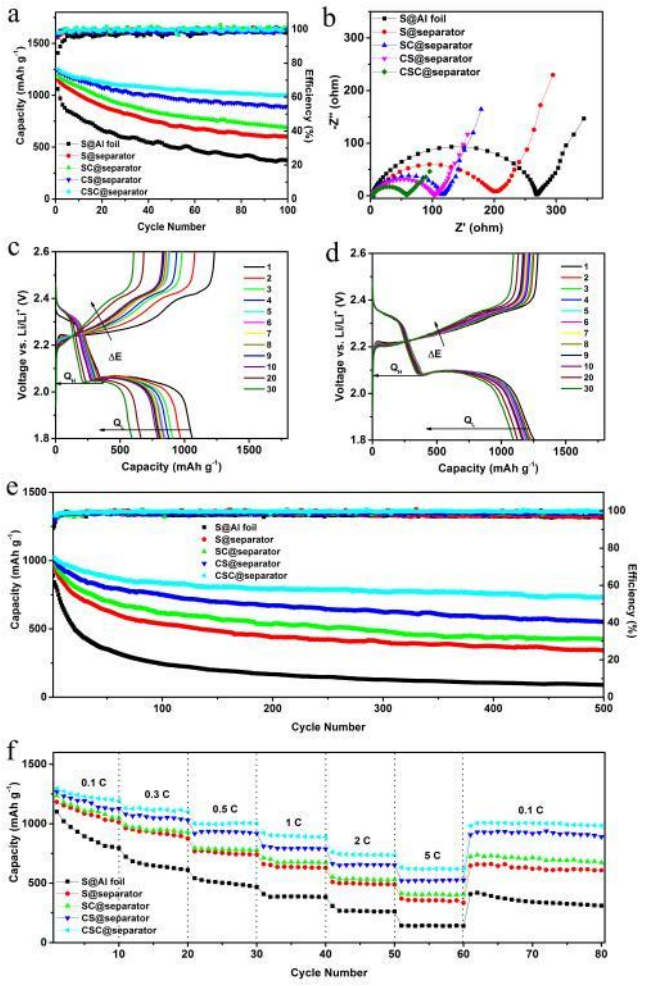

Figure 2. a) Cycling stability (0.2 C, 1 C = 1000 mA g^{-1}) and b) electrochemical impedance spectroscopy of Li-S cells using S@Al foil and a series of integrated electrodes. Discharge-charge profiles for selected cycles of Li-S cells with c) S@Al foil and d) CSC@separator electrodes. e) Long-term cycling performance and f) rate capability of Li-S cells with S@Al foil, and a series of integrated electrodes at 0.6C.

The long-term cycling stability of the CSC@separator electrode was studied at 0.6C for 500 cycles (Figure 2e), and the capacity stabilized around 730 mAh g^{-1}, corresponding to 71.2% capacity retention and a small capacity fading of only 0.058% per cycle. It should be noted that our integrated CSC@separator electrode prepared from commercial sulfur and

Super P can still exhibit such a good electrochemical performance. If nanostructured sulfur materials, such as sulfur-TiO_2 yolk shell nanoarchitecture,[19] can be used to fabricate the sulfur layer in our novel configuration design, much superior electrochemical performance could definitely be obtained. Moreover, the highly reversible CSC@separator electrode delivered capacities of 1220, 1120, 1000, 900, 740, and 620 mAh g^{-1} at 0.1, 0.3, 0.5, 1, 2, and 5C, respectively, confirming the excellent rate capability (Figure 2f). It should be also pointed out that the introduction of the double carbon coating layers does not notably degrade the lithium ion conductivity, as confirmed by the similar diffusion coefficients of S@Al foil and the CSC@separator electrodes (Figure S2).

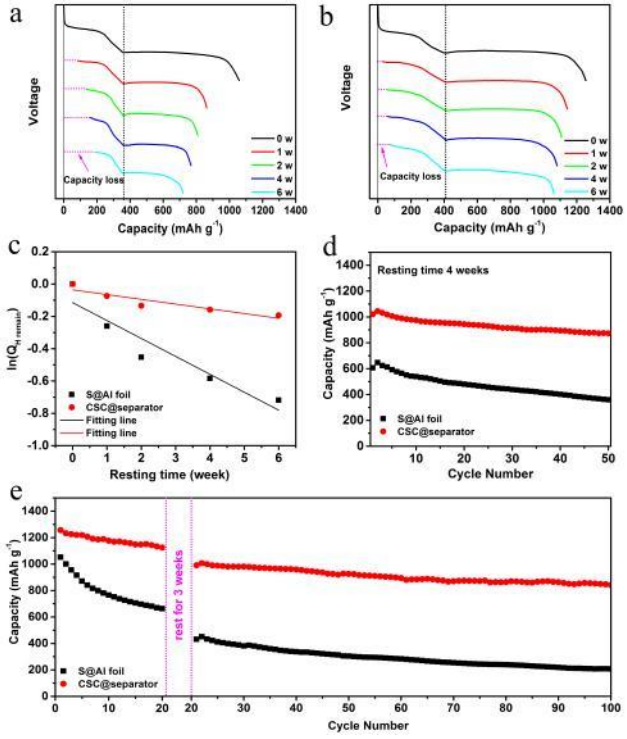

Figure 3. a) Initial discharge profiles of Li-S cells with S@Al foil and b) CSC@separator electrodes after different open-circuit durations at current density of 0.2 C. c) Natural logarithm of the retention rate of upper plateau discharge capacity as a function of resting time for calculating the self-discharge constant. d) Cycling performances of the cells containing S@Al foil and CSC@separator electrodes after 4 weeks storage and e) with 3 weeks resting time after 20 cycles at 0.2 C.

The integrated CSC@separator electrode also offers notable improvement of the self-discharge behaviour in Li-S batteries. The severe self-discharge behavior mainly arises from the dissolution of sulfur during long-term storage, as can be clearly observed in the cells with S@Al foil electrode (Figure 3a and Figure S7), causing a capacity loss of 37.8% of its original capacity after a 2 weeks storage. However, the cell with CSC@separator electrode shows almost repeated discharge curves and low capacity loss of 14.5% (Figure 3b), indicating that the sulfur materials are well controlled within the double carbon layers, resulting in low self-discharge constant K_s of 0.0293 per week (Figure 3c and Table S1). The static electrochemical stability of the S@Al foil electrode and the CSC@separator electrodes is shown in Figure 3d, e. After resting for 4 weeks, the cell with CSC@separator electrode still shows good cycling stability with high initial capacity retention of 81.3%. In addition, the CSC@separator electrode after 20 cycles delivered much higher reversible capacity after resting for 3 weeks. The significantly improved static capacity retention indicates that the double carbon coating layer in the sandwich structure serves as a protective layer, preventing the sulfur material from dissolving into the electrolyte and thus eliminating the severe self-discharge problem that occurs in the conventional Li-S cells.

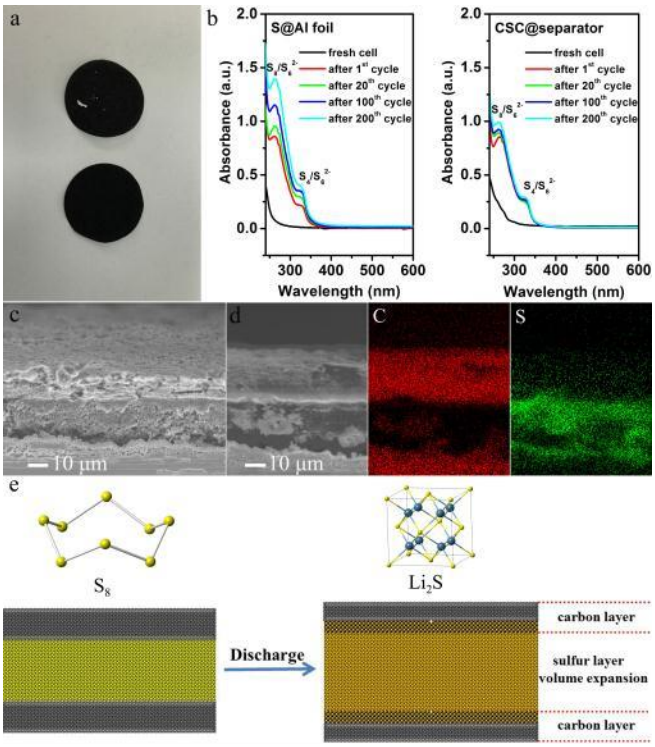

Figure 4. a) Digital photographs of S@Al foil (top) and CSC@separator electrodes (bottom) after 100 cycles. b) UV-vis absorption spectra of DOL/DME solution with S@Al foil electrode and CSC@separator electrode at various cycle numbers. c) SEM image and d) elemental mapping of the cross-section of CSC@separator after 100 cycles. e) Schematic illustration of polysulfide diffusion, with trapping between the carbon layers.

Figure 4a presents digital photographs of S@Al foil and CSC@separator electrodes after 100 cycles. A small amount of active materials exfoliated from S@Al foil electrode. In contrast, the CSC@separator electrode maintained a good appearance, without any obvious exfoliation or changes, indicating good structural stability. Furthermore, the cycled S@Al foil and CSC@separator electrodes were examined by ultraviolet-visible (UV-vis) absorption spectroscopy. The color of the DOL/DME solutions for the S@Al foil electrodes changed from colorless to yellow with cycle number, while no noticeable color change for the CSC@separator electrodes (Figure S8). The similar intensities of the peaks for the CSC@separator electrodes at different cycles indicate similar content of polysulfides in the electrolyte, confirming a low rate of polysulfide diffusion and effective absorption by the double carbon layers (Figure 4b). The morphology of the cycled S@Al foil and CSC@separator electrodes was studied by SEM (Figure S9). After 100 cycles, the surface of the S@Al foil electrode became denser and large

particle aggregation can be clearly observed. The elemental mapping and energy-dispersive X-ray (EDX) spectroscopy results revealed that the particle aggregates are rich in sulfur. In contrast, the CSC@separator electrode shows no obvious changes, and no particle aggregation and a weak signal of sulfur, suggesting that the diffusion of polysulfide is controlled within the two carbon layers. To further confirm the effects of the carbon layer towards suppressing the diffusion of the polysulfides, a cross-sectional SEM image and a schematic illustration of polysulfide diffusion in the CSC@separator electrode are shown in Fig. 4c-e. The sandwich structure of the CSC@separator electrode is still well maintained after 100 cycles, demonstrating the excellent structural stability of the integrated electrode, which could control the diffusion of polysulfides, buffer the volume changes during cycling, and maintain the integrity of the whole electrode.

To further understand why the integrated electrode could delivery more stable capacity than the conventional S@Al foil electrode, the cycling performance of a half-covered S@separator electrode was tested (Figure S10). Apparently, there is a small amount of Super P in the S@separator electrode, which could easily disperse into the nanopores of the separator and act as a complete physical barrier to prevent polysulfide diffusion to the anode side for a fully covered S@separator electrode. The uncovered area, however, in the half-covered S@separator electrode, results in poor cycling performance. Commonly, no matter how sophisticated the nanostructured sulfur cathode is in a conventional Li-S cell, it is inevitable that small amounts of polysulfides will dissolve into the electrolyte and then diffuse across the nanoporous separator, leading to the capacity fading. In our design, however, the dissolved polysulfides must travel through the carbon coating layer before the separator, fully encountering the absorption effect of the carbon layer. The carbon layers could serve as effective barriers to control the diffusion of the polysulfides and keep them within the cathode region, eliminating the shuttle effect and self-discharge behaviour to a large extent. The shuttle factor for the CSC@separator electrode is 0.067, much lower than that for the S@Al foil electrode (0.42, Table S2).

In summary, for the first time, we have successfully designed and prepared a unique flexible cathode architecture consisting of a carbon/sulfur/carbon sandwich structure coated directly on a PP separator via the doctor blade method. The CSC@separator cathode delivered a high reversible capacity of 730 mAh g^{-1} over 500 cycles, with capacity decay as small as 0.058% per cycle and a low self-discharge constant of 0.0293 per week. Improved performance is attributed to the enhanced electronic conductivity, toleration of volume expansion, and control of the polysulfide diffusion of the unique integrated sandwich-structured electrode. Together with the simple and scalable nature of its fabrication, our integrated sandwich structured electrode is highly promising for practical application in Li-S batteries.

Acknowledgements

Financial support provided by the Australian Research Council (ARC) through an ARC Discovery project (DP1094261) is gratefully acknowledged. Moreover, the authors would like to thank Dr Tania Silver for critical reading of the manuscript and valuable remarks.

Keywords: lithium-sulfur batteries • integrated flexible cathode • shuttle effect • self-discharge

[1] S. E. Cheon, S. S. Choi, J. S. Han, Y. S. Choi, B. H. Jung, H. S. Lim, *J. Electrochem. Soc.* **2004**, 151, A2067-A2073.
[2] X. L. Ji, K. T. Lee, L. F. Nazar, *Nat. Mater.* **2009**, 8, 500-506.
[3] P. G. Bruce, S. A. Freunberger, L. J. Hardwick, J. M. Tarascon, *Nat. Mater.* **2012**, 11, 19-29.
[4] Y. Yang, G. Y. Zheng, S. Misra, J. Nelson, M. F. Toney, Y. Cui, *J. Am. Chem. Soc.* **2012**, 134, 15387-15394.
[5] Z. Li, J. T. Zhang, X. W. Lou, *Angew. Chem. Int. Ed.* **2015**, 54, 12886-12890; *Angew. Chem.* **2015**, 127, 13078-13082.
[6] N. Jayaprakash, J. Shen, S. S. Moganty, A. Corona, L. A. Archer, *Angew. Chem. Int. Ed.* **2011**, 50, 5904-5908; *Angew. Chem.* **2011**, 123, 6026-6030.
[7] H. L. Wang, Y. Yang, Y. Y. Liang, J. T. Robinson, Y. G. Li, A. Jackson, Y. Cui, H. J. Dai, *Nano. Lett.* **2011**, 11, 2644-2647.
[8] C. Zhang, H. B. Wu, C. Yuan, Z. Guo, X. W. Lou, *Angew. Chem. Int. Ed.* **2012**, 51, 9592-9595; *Angew. Chem.* **2012**, 124, 9730-9733.
[9] Q. Pang, J. T. Tang, H. Huang, X. Liang, C. Hart, K.C. Tam, L.F. Nazar, *Adv. Mater.* **2015**, 27, 6021-6028.
[10] L. N. Wang, Y. Zhao, M. L. Thomas, H. R. Byon, *Adv. Funct. Mater.* **2014**, 24, 2248–2252.
[11] J. X. Song, M. L. Gordin, T. Xu, S. R. Chen, Z. X. Yu, H. Sohn, J. Lu, Y. Ren, Y. H. Duan, D. H. Wang, *Angew. Chem. Int. Ed.* **2015**, 54, 4325-4329; *Angew. Chem.* **2015**, 127, 4399-4403.
[12] Q. Sun, X. Fang, W. Weng, J. Deng, P. N. Chen, J. Ren, G. Z. Guan, M, Wang, H. S. Peng, *Angew. Chem. Int. Ed.* **2015**, 54, 10539-10544; *Angew. Chem.* **2015**, 127, 10685-10690.
[13] M. Q. Zhao, Q. Zhang, J. Q. Huang, G. L. Tian, J. Q. Nie, H. J. Peng, F. Wei, *Nat. Commun.* **2014**, 5, 3410.
[14] J. P. Rong, M. Y. Ge, X. Fang, C. W. Zhou, *Nano Lett.* **2014**, 14, 473–479.
[15] J. L. Wang, Y. S. He, J. Yang, *Adv. Mater.* **2015**, 27, 569-575.
[16] L. F. Xiao, Y. L. Cao, J. Xiao, B. Schwenzer, M. H. Engelhard, L. V. Saraf, Z. M. Nie, G. J. Exarhos, J. Liu, *Adv. Mater.* **2012**, 24, 1176-1181.
[17] K. Park, J. H. Cho, J. H. Jang, B. C. Yu, A. T. De La Hoz, K. M. Miller, C. J. Ellison, J. B. Goodenough, *Energy Environ. Sci.* **2015**, 8, 2389-2395.
[18] X. Liang, A. Garsuch, L. F. Nazar, *Angew. Chem. Int. Ed.* **2015**, 54, 3907-3911; *Angew. Chem.* **2015,** 127, 3979-3983.
[19] Z. W. Seh, W. Y. Li, J. J. Cha, G. Y. Zheng, Y. Yang, M. T. McDowell, P. C. Hsu, Y. Cui, *Nat. Commun.* **2013**, 4, 1331.
[20] Q. Pang, D. Kundu, M. Cuisinier, L. F. Nazar, *Nat. Commun.* **2014**, 5, 4759.
[21] Z. Liang, G. Y. Zheng, W. Y. Li, Z. W. Seh, H. B. Yao, K. Yan, D. S. Kong, Y. Cui, *ACS Nano* **2014**, 8, 5249-5256.
[22] K. E. Hendrickson, L. Ma, G. Cohn, Y. Y. Lu, L. A. Archer, *Adv. Sci.* **2015**, 2, 1500068.
[23] Y. S. Su, A. Manthiram, *Nat. Commun.* **2012**, 3, 1166.
[24] Y. S. Su, A. Manthiram, *Chem. Commun.* **2012**, 48, 8817-8819.
[25] J. Q. Huang, B. A. Zhang, Z. L. Xu, S. Abouali, M. A. Garakani, J. Q. Huang, J. K. Kim, *J. Power Sources* **2015**, 285, 43-50.
[26] X. F. Wang, Z. X. Wang, L. Q. Chen, *J. Power Sources* **2013**, 242, 65-69.
[27] S. H. Chung, A. Manthiram, *Chem. Commun.* **2014**, 50, 4184-4187.
[28] J. Q. Huang, Q. Zhang, H. J. Peng, X. Y. Liu, W. Z. Qian, F. Wei, *Energy Environ. Sci.* **2014**, 7, 347-353.
[29] S. H. Chung, A. Manthiram, *Adv. Mater.* **2014**, 26, 7352-7357.
[30] J. Q. Huang, T. Z. Zhuang, Q. Zhang, H. J. Peng, C. M. Chen, F. Wei, *ACS Nano* **2015**, 9, 3002-3011.

COMMUNICATION

An integrated flexible sulfur cathode consisting of a carbon/sulfur/carbon sandwich structure coated on a polypropylene separator was prepared by the doctor-blade method. This sulfur cathode could enhance the electronic conductivity, toleration of volume expansion, and control of the polysulfide diffusion, thereby improving the electrochemical performance of lithium-sulfur batteries.

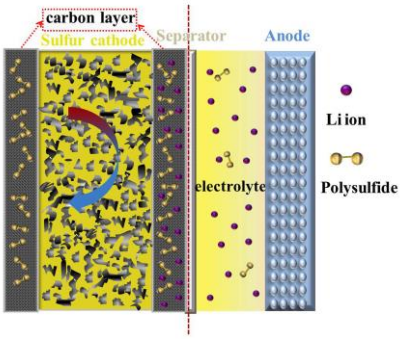

*Hongqiang Wang, Wenchao Zhang, Huakun Liu, and Zaiping Guo**

Page No. – Page No.

A Strategy for Configuration of an Integrated Flexible Sulfur Cathode for High-Performance Lithium-Sulfur Batteries

Supporting Information

Experimental Section

Preparation of sulfur active material

Commercial conductive carbon (Super P) and sulfur were mixed together in weight ratios of 15:85 and 70:30, respectively, and heated to 160 °C in a sealed stainless steel autoclave for 24 h to facilitate sulfur diffusion into the carbon host. Finally, the content of sulfur in the composite is determined by thermal gravimetric analysis (81% and 63 %, respectively).

Fabrication of CSC@separator cathode

The integrated CSC@separator electrode was fabricated by the slurry casting technique on one side of a Celgard 2400 polypropylene (PP) separator. The slurry C for the carbon coating layer was prepared by mixing Super P and polyvinylidene difluoride (PVDF) in N-methyl-2-pyrrolidinone (NMP). The slurry S for the sulfur layer was synthesized by mixing sulfur active material (81%, sulfur content) and binder without any additional conductive carbon in the weight ratio of 85:15. In a typical procedure, slurry C was coated on one side of the PP separator using blade coating method. After drying at 60 ^{o}C for 24 h, slurry S was coated on the surface of the carbon layer, and then another carbon layer was coated on the surface of sulfur layer after drying to obtain the integrated CSC@separator cathode. The weight of two carbon coating layers is only 0.38-0.52 mg cm^{-2}, much lighter than the weight of the

sulfur layer at 1.0-1.4 mg cm^{-2}. Even including the weight of the carbon coating layers, the content of sulfur in the whole electrode is still around 50%.

Fabrication of S@Al foil cathode

For comparison, a conventional S@Al foil sulfur electrode was also prepared by the casting method. A slurry was made of the sulfur active material (63%, sulfur content), Super P, and binder in a certain weight ratio to make sure the same content of sulfur as in the CSC@separator electrode.

Characterization

The morphologies and structures of the as-prepared CSC@separator and S@Al foil electrodes were analysed by field-emission scanning electron microscopy (FESEM; JEOL JSM-7500FA). The load-strain curves of the pristine separator and the CSC@separator were tested using Tensile & Compression Testers (INSTRON 5943). The contents of polysulfides in the DOL/DME solutions in the cells with these electrodes after different cycle number were characterized with a UV-3600 spectrophotometer (Shimadzu).

Electrochemical measurements

Coin-type (CR2032) cells were assembled in an argon-filled glove box. The electrolyte used was 1 M lithium bis(trifluoromethanesulfonyl)imide in a solvent mixture of 1,3-dioxolane (DOL): dimethoxyethane (DME) (1:1, v/v), containing 2 wt% $LiNO_3$. Cyclic voltammetry (CV) and electrochemical impedance spectroscopy (EIS) measurements were performed on a Biologic VMP3 electrochemical workstation at

different scan rates. The coin cells were galvanostatically charged-discharged between 1.8 and 2.6 V (vs. Li/Li^+) by using a cell test instrument (CT2001A, LAND, China). The self-discharge behaviour of the cells employing S@Al foil and CSC@separator electrodes was measured by testing the first discharge capacity of the cells after different resting time.

Table S1. Self-discharge constant of Li-S cells with different electrodes.

Electrode	Self-discharge constant K_s (per week)
S@Al foil	0.1107
CSC@separator	0.0293

The self-discharge constant of cells containing S@Al foil and CSC@separator electrodes can be calculated by the following equation:

$$\ln(Q_{H\,remain}) = \ln\left(\frac{Q_H}{Q_{H^0}}\right) = -\mathrm{K_s} \times \mathrm{T_R} \quad (1)$$

Q_H and Q_H^o are the upper plateau discharge capacity of Li-S cells without a resting time and the initial upper plateau discharge capacity of the cells after a period of storage time, respectively. K_s is the self-discharge constant, while T_R stands for the resting time (weeks).

Table S2. Calculation of shuttle factor for Li-S cells using the conventional S@Al foil and CSC@separator electrodes.

Electrode	Shuttle Factor
S@Al foil	0.4196
CSC@separator	0.0666

The shuttle factor suggested by Mikhaylik and Akridge[1] is defined to reflect the extent of the shuttle effect. The shuttle factor is expressed as:

$$f = k_s \cdot Q_H / I \quad (2)$$

Where k_s is the heterogeneous reaction constant related to polysulfide diffusion and reaction, Q_H is the theoretical charge/discharge capacity of the high plateau, and I is the charge/discharge current. Based on a previous report[1], the relationship between the Coulombic efficiency and the shuttle factor can be expressed as follows:

$$C_{eff} = \frac{2 + (ln(1+f))/f}{2 - (ln(1-f))/f}$$

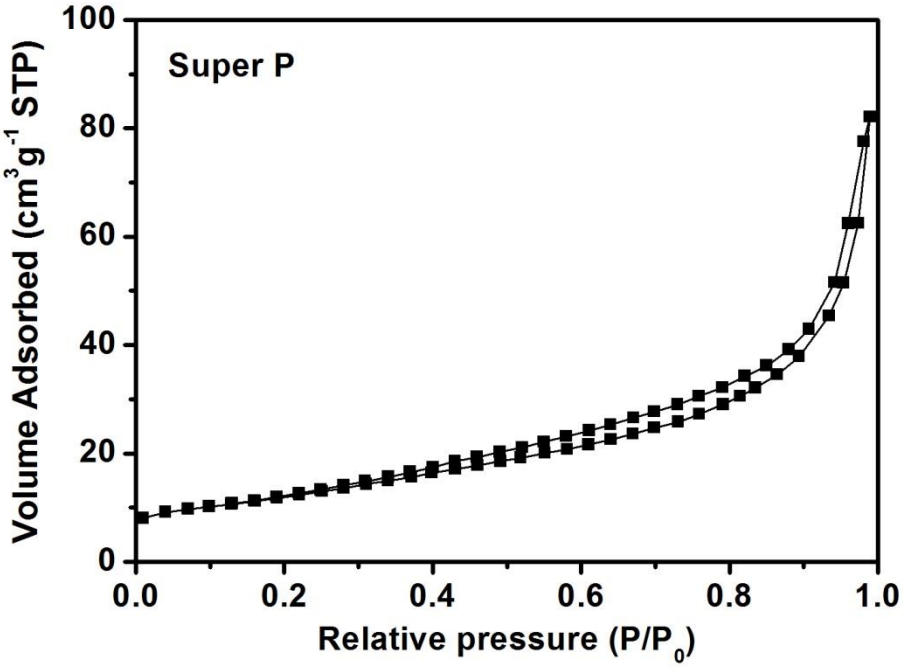

Fig. S1. N_2 isotherm of Super P.

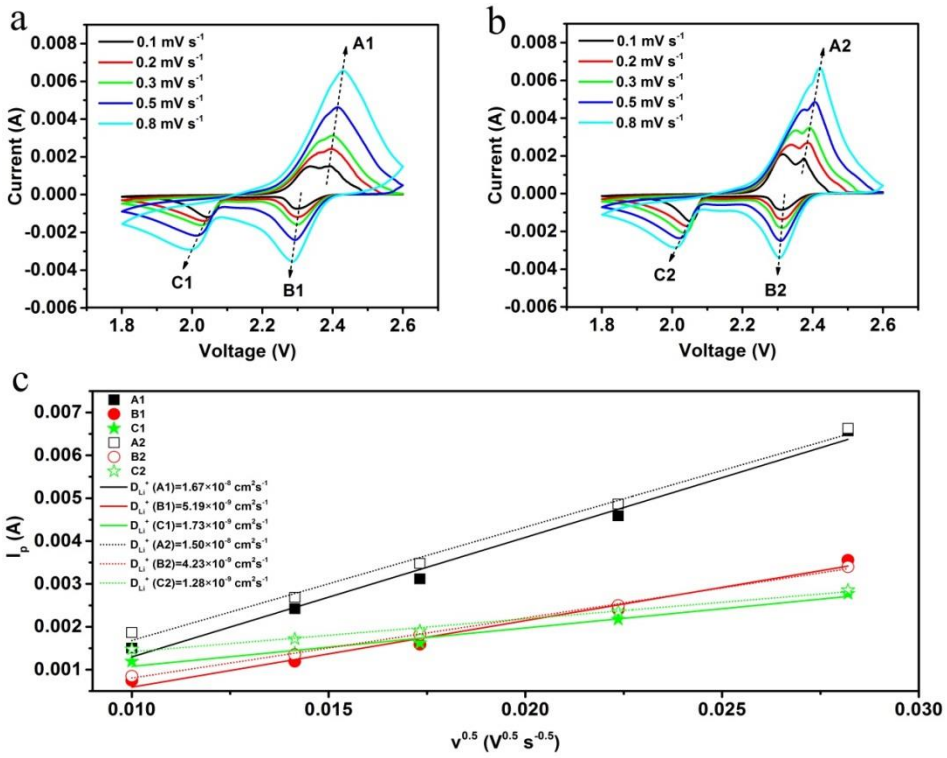

Fig. S2. CV curves at different scan rates of Li-S cells with (a) S@Al foil and (b) CSC@separator electrodes. (c) Peak currents versus $V^{0.5}$ $s^{-0.5}$ and the corresponding linear fits.

The lithium-ion diffusion coefficient (D_{Li}^{+}) can be calculated based on the Randles-Sevcik equation:

$$i_p = 0.4463nF\sqrt{\frac{nFD}{RT}}AC\sqrt{v}$$

Where i_p represents peak current, n is the number of electrons, F is the Faraday constant, R is the gas constant, T is the temperature, A is the surface area of the electrode, D is the diffusion coefficient, C stands for the concentration of lithium-ions in the electrolyte, and v is the voltage scanning rate.

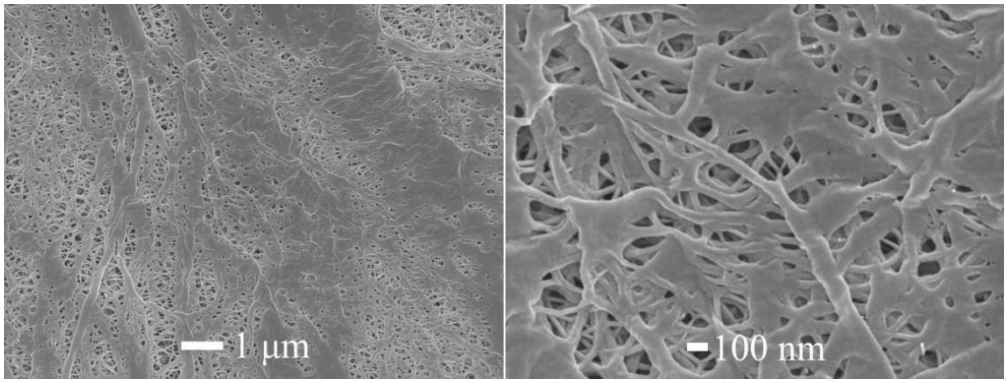

Fig. S3. SEM images of CSC@separator electrode on the anode side.

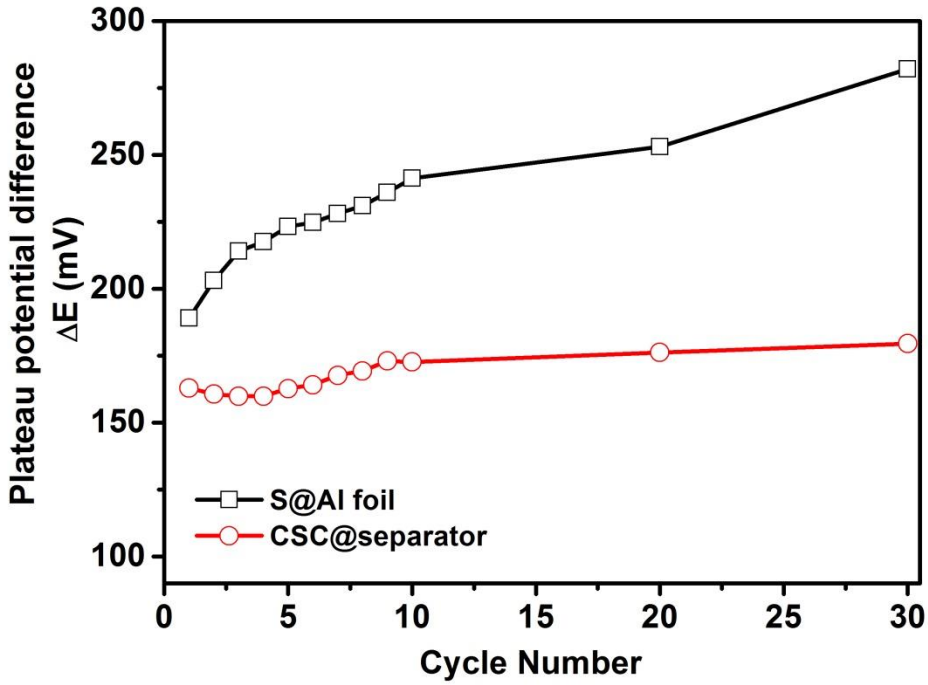

Fig. S4. Potential difference (ΔE) between the charge and discharge plateaus at different cycle numbers for cells containing S@Al foil and CSC@separator electrodes.

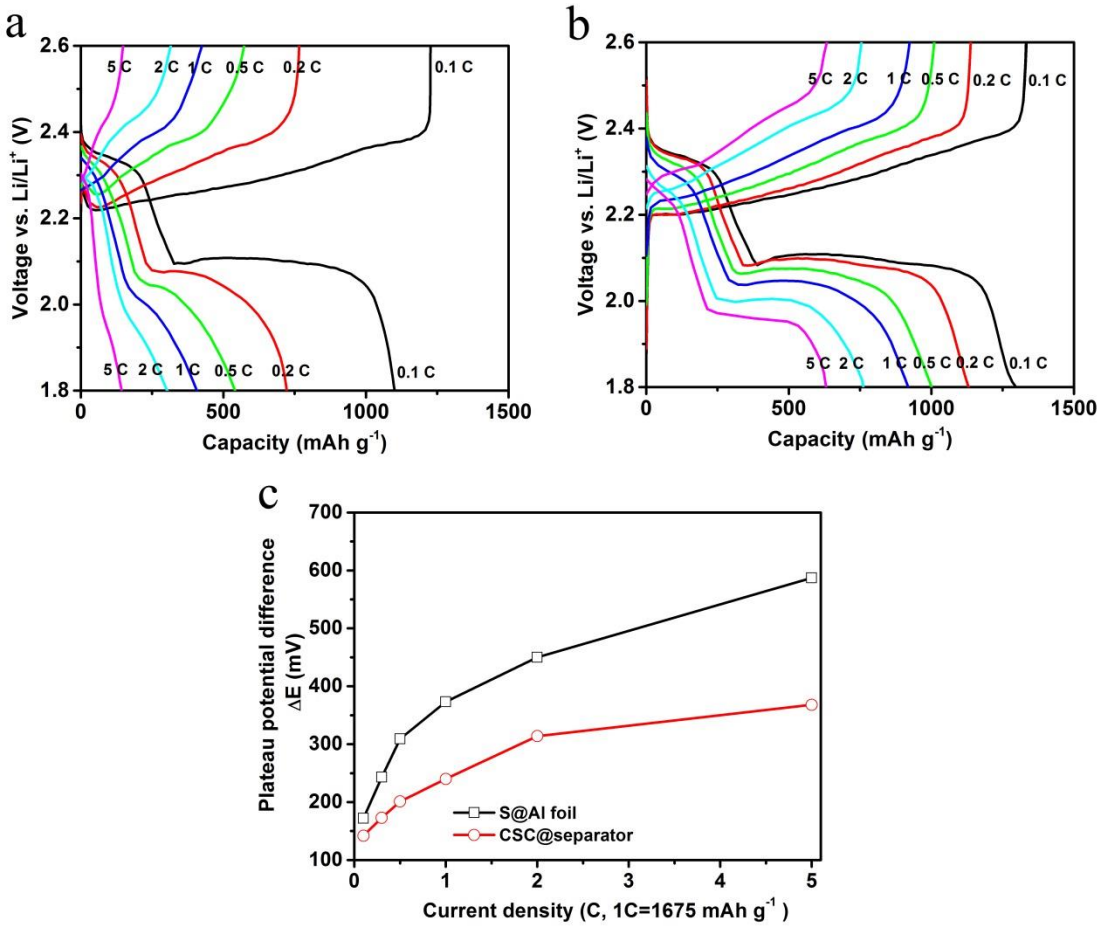

Fig. S5. Discharge-charge curves of Li-S cells with (a) S@Al foil and (b) CSC@separator electrodes at different current densities. (c) Potential difference (ΔE) between the charge and discharge plateaus at different current densities.

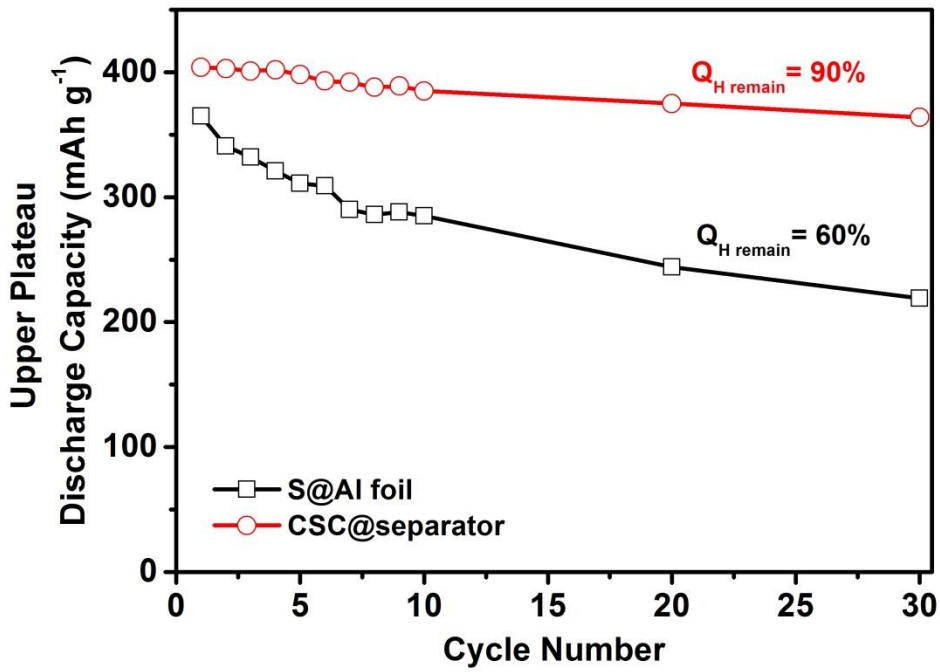

Fig. S6. Upper plateau discharge capacity of cells using S@Al foil and CSC@separator electrodes at different cycle numbers.

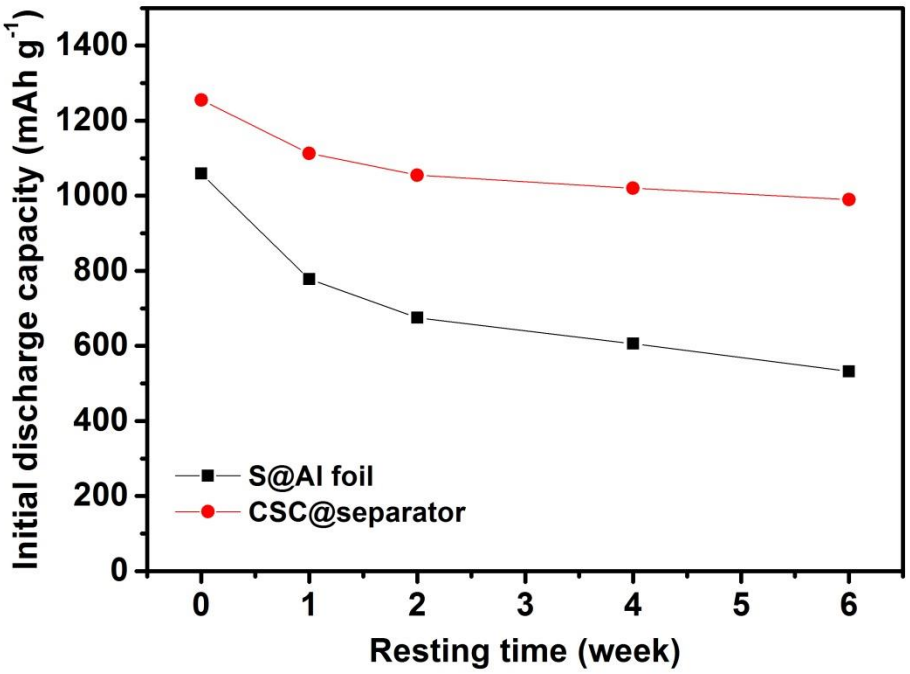

Fig. S7. Initial discharge capacity of Li-S cells with S@Al foil and CSC@separator electrodes after different resting times.

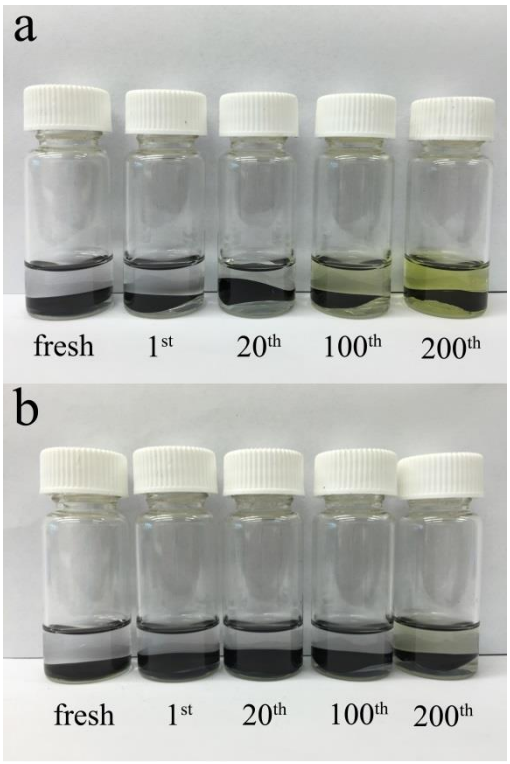

Fig. S8. Typical colours of the DOL/DME solutions with cycled (a) S@Al foil electrodes and (b) CSC@separator electrodes.

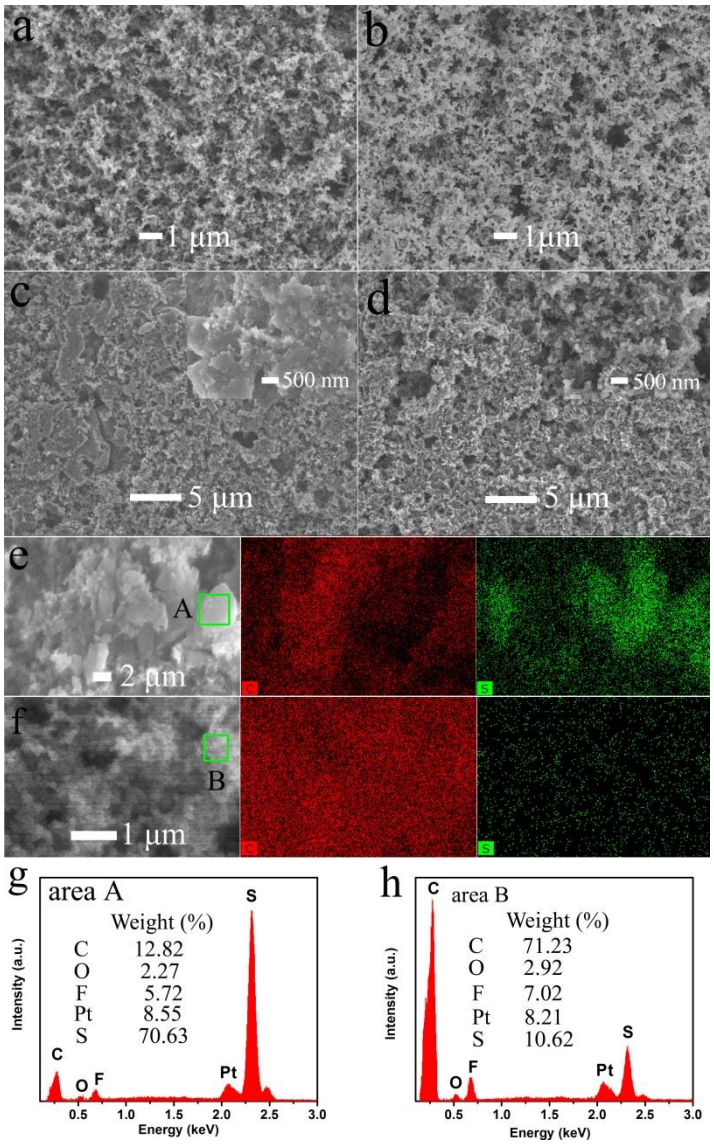

Fig. S9. SEM images of the S@Al foil electrode (a) before and (c) after 100 cycles, and of the CSC@separator electrode (b) before and (d) after 100 cycles, and corresponding elemental mapping of carbon and sulfur for (e) S@Al foil and (f) CSC@separator electrodes after 100 cycles. EDX spectra for selected areas of cycled (g) S@Al foil electrode and (h) CSC@separator electrode.

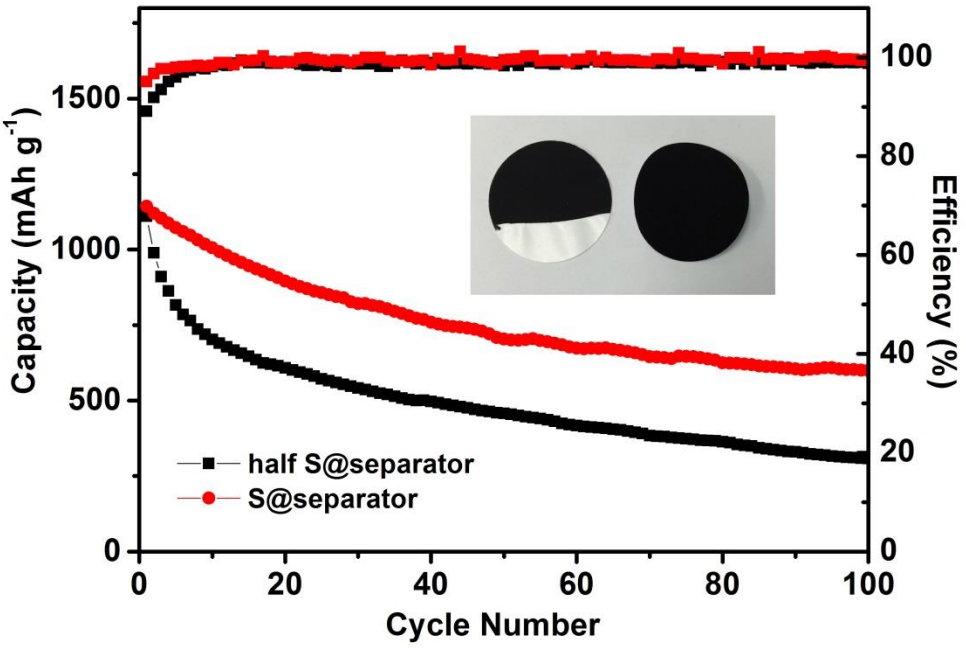

Fig. S10. Comparison of cycling performance of Li-S cells with S@separator and half S@separator electrodes.

Reference

[1] Y. V. Mikhaylik, J. R. Akridge, *J. Electrochem. Soc.* **2004**, 151, A1969-A1976.